CrystEngComm

Cite this: *CrystEngComm*, 2011, **13**, 4831

www.rsc.org/crystengcomm

COMMUNICATION

A facile template-free route to fabricate highly luminescent mesoporous gadolinium oxides†

Weihua Di, Xinguang Ren,* Ligong Zhang, Chunxu Liu and Shaozhe Lu

Received 12th April 2011, Accepted 24th May 2011
DOI: 10.1039/c1ce05435j

This work first demonstrates a simple template-free approach for the preparation of nanoporous rare earth oxides with well-defined mesopores, large pore size and specific surface area, and high photoluminescence quantum yield.

Recently, luminescent rare-earth-based nanoparticles have been demonstrated as a promising new class of biological fluorescent labels because of their unique photophysical properties, such as large Stokes shift, narrow emission bandwidths, long fluorescence lifetime, high emission quantum yield, inherent photostability and rather low cytotoxicity.[1] Luminescent nanoporous materials are potential candidates for *in vitro* and *in vivo* targeted drug/gene delivery vehicles because of their well-defined interior voids, large surface area, stability, surface permeability and especially the simultaneous monitoring of the actions *via* luminescence.[2]

Currently, the synthetic strategies for the fabrication of pore structures mostly involve the utilization of various removable templates, including soft ones such as surfactants, emulsion droplets, micelles, vesicles, ionic solvents, and gas bubbles, and hard ones, such as polymers, silica, carbon, metal oxides and metallic cores.[3] In general, the template-based synthetic methods involve multistep procedures, and sometimes require stringent synthesis conditions. In some cases, some toxic surfactants or solvents are needed to add into the reaction system, which renders the final material with significant toxicity.[4] At present, the luminescent porous materials are commonly constructed through a composite/hybrid structure, such as the anchoring of the fluorophore groups on the mesoporous material and coating of luminescent particles with a porous layer.[5] Clearly, these processes for obtaining such a luminescent porous composite structure are complicated, and also not suitable for large-scale production. Therefore, it is still a challenge to prepare single-phased luminescent porous materials *via* a simple, economical and green synthetic process.

Herein, we presente a facile strategy to fabricate porous gadolinium oxides (Gd_2O_3) by a solid-state-chemistry based thermal decomposition process of rare earth complex sources. It is demonstrated that this new strategy provides a simple template-free approach for cost-effective and scalable preparation of nanoporous rare earth oxides with well-defined mesopores, large pore size and high enough specific surface area. Furthermore, the obtained mesoporous rare earth oxides with lanthanide doping exhibit a high luminescence quantum yield.

The precursor to generate porous gadolinium oxides, gadolinium hydroxylcarbonate ($Gd(OH)CO_3 \cdot H_2O$:Eu), was prepared *via* a urea-based homogeneous precipitation method (Experimental section, ESI†), in which urea serves as a precipitation agent for metal cations due to self-decomposition into OH^- and CO_3^{2-} at elevated temperatures (>83 °C). The urea-based precipitation is a simple and general route for the preparation of rare earth hydroxylcarbonate that was first developed by Matijevic and Hsu.[6] X-Ray diffraction (XRD) measurements revealed that the as-prepared precursor material is amorphous. Elemental analysis and Fourier transform infrared (FTIR) spectroscopy confirmed that the chemical composition of the as-prepared precursor is $Gd(OH)CO_3 \cdot H_2O$:Eu (Table S1 and Fig. S1, ESI†), which is consistent with the pioneering work of Matijevic and Hsu[6] and the recent work by Lechevallier's group.[7]

The idea of this work was inspired by examining the thermogravimetric analysis (TGA) curve (Fig. 1) of the precursor $Gd(OH)CO_3 \cdot H_2O$:Eu. The weight loss of $Gd(OH)CO_3 \cdot H_2O$:Eu occurs in

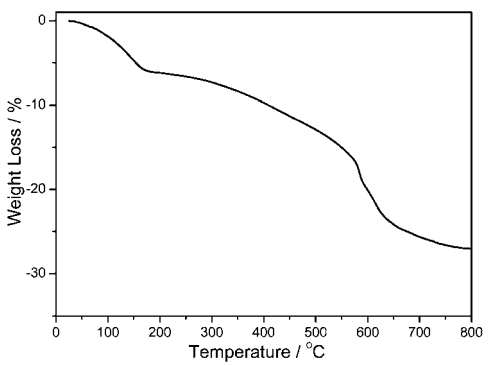

Fig. 1 Thermogravimetric analysis curve of the precursor $Gd(OH)CO_3 \cdot H_2O$:Eu in air, indicating a two-step thermal decomposition process in the range 200–750 °C.

Key Laboratory of Excited-state Processes, Changchun Institute of Optics, Fine Mechanics and Physics, Chinese Academy of Sciences, 3888 Eastern South Lake Road, Changchun, 130033, P.R. China. E-mail: xgrenchina@ciomp.ac.cn

† Electronic supplementary information (ESI) available: Details of experimental procedures on the preparation of the precursor $Gd(OH)CO_3 \cdot H_2O$:Eu and mesoporous Gd_2O_3:Eu, characterizations (including FT-IR, N_2 adsorption–desorption isotherm, photoluminescence and quantum yield), and supporting images. See DOI: 10.1039/c1ce05435j

three steps. The first one, before 150 °C, was associated with the release of about 5 wt% residual water and ethanol adsorbed on the powder surface due to the storage of the material in air and the washing procedure, respectively. The second one (200–550 °C) is related to the removal of water molecules due to the dehydration of hydrated compounds and the self-condensation of hydroxyl groups (O–H). This is confirmed by the FTIR spectrum of the sample calcinated at 550 °C (Fig. S1(b), ESI†), in which the characteristic absorptions of hydration water and hydroxyl groups almost disappear completely, compared to that of the as-prepared $Gd(OH)CO_3 \cdot H_2O$. The third weight loss originates from the release of CO_2 molecules that is also confirmed by the FTIR spectrum of the sample calcinated at 750 °C (Fig. S1(c), ESI†), in which we observed the disappearance of the characteristic vibrations of CO_3^{2-}.

Our curiosity was driven by a question: what are the composition, morphology, structure, and properties of the final product obtained after thermal treatments? Based on such curiosity, we first checked the morphology of samples before and after calcination. Fig. 2 presents typical transmission electron microscopy (TEM) images of the samples before and after calcination. The as-prepared $Gd(OH)CO_3 \cdot H_2O$:Eu particles appear spherical and nearly monodispersed (Fig. 2a and b). The size distribution plot based on the analysis of 100 particles from TEM observations indicates that the spherical particle size ranges from 130 to 170 nm with an average diameter of 150 nm and a standard deviation of ±10.6% (Fig. S2, ESI†).

The particles calcinated at 750 °C still maintain spherical shape and original size (Fig. 2c) in spite of the high total weight loss up to 30% (Fig. 1). This implies there will be a large amount of porosity left within the particles. As observed from a typical high resolution TEM image (Fig. 2d), a spherical particle contains tens of small sized nanoparticles (~15 nm, dark regions) that are separated by tens of pores (light regions). These pores were randomly arranged but distributed homogenously throughout the whole particle, and they are large enough (10–15 nm) and uniform with a narrow size distribution. Surprisingly, the framework of the as-prepared precursor particles did not collapse while the mesopore structures were created as a result of the gases burning out during calcination. As a matter of fact, the key to maintain the original particle morphology and create the mesopore structures within the particle is to control the decomposition process at a low heating rate. The rapid heating-up can lead to vigorous gas burst-out, which might destroy the regular morphology of the as-prepared particles and cause the remarkable shrinkages. In our experiment, the heating rate is controlled to be low enough (2 °C min^{-1}) to allow a relatively slow release of gases, which efficiently prevents the remarkable shrinkage of materials and thus leads to the formation of uniform pores surrounding those separated small sized nanoparticles within the original particles. Simultaneously, those small sized nanoparticles separated by the pores are converted and crystallized into gadolinium oxides from the amorphous $Gd(OH)CO_3 \cdot H_2O$:Eu upon thermal treatment, as revealed by XRD (Fig. 2f). Therefore, the thermal decomposition of the precursor $Gd(OH)CO_3 \cdot H_2O$:Eu at a temperature up to 750 °C yields uniform mesoporous and highly crystallized gadolinium oxides.

The nitrogen adsorption–desorption isotherm, as shown in Fig. 3, provides further evidence for the formation of mesoporous Gd_2O_3:Eu obtained by the thermal decomposition of precursor $Gd(OH)CO_3 \cdot H_2O$:Eu. The isotherm can be classified as a type IV, which is the characteristic of the disordered mesoporous structure. The Brunauer–Emmett–Teller (BET) specific surface area (S_{BET}) calculated from the linear part of the nitrogen adsorption isotherm plot was increased from 10 $m^2 g^{-1}$ for $Gd(OH)CO_3 \cdot H_2O$:Eu to 118 $m^2 g^{-1}$ for the mesoporous Gd_2O_3:Eu. The average pore diameter calculated from the nitrogen adsorption isotherm by the Barrett–Joyner–Halenda (BJH) method was 12.6 nm and the pore size distribution is narrow (inset of Fig. 3). The BET measurement of Gd(OH)

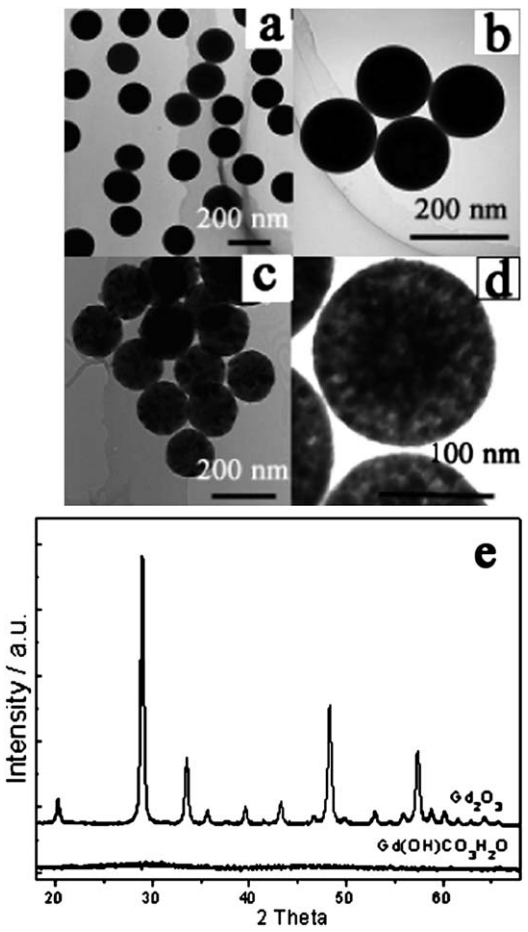

Fig. 2 TEM images of the as-prepared $Gd(OH)CO_3 \cdot H_2O$:Eu before (a and b) and after calcination (c and d); (e) the corresponding XRD patterns of samples before and after the treatment.

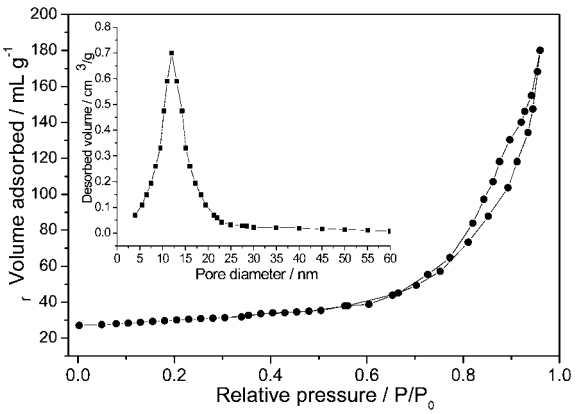

Fig. 3 Nitrogen adsorption–desorption isotherm of mesoporous Gd_2O_3:Eu. The inset shows the corresponding pore size distribution curve.

$CO_3 \cdot H_2O$:Eu shows that no hysteresis-loop in the nitrogen adsorption–desorption isotherm was observed and that no significant peak was seen from the pore size distribution curve (Fig. S4, ESI†), indicating that no mesopores exist in the as-prepared precursor, as observed by TEM (Fig. 2b). The difference observed from both samples before and after calcination further confirms that the mesopores within a spherical Gd_2O_3:Eu particle are formed by the gases burning out during the thermal decomposition of $Gd(OH)CO_3 \cdot H_2O$:Eu. It is demonstrated that this new strategy provides a simple template-free approach for the preparation of nanoporous rare earth oxides with well-defined mesopores, large pore size and high specific surface area.

Rare earth oxides have been shown to be a useful host lattice for lanthanide ions to produce phosphors emitting a variety of colors (*e.g.* Gd_2O_3:Eu/Tb, Y_2O_3:Yb,Er).[8] Eu^{3+}-doped samples with an optimized dopant concentration (5 mol%) were prepared for the luminescence investigations. The doping of Eu^{3+} does not affect the morphology of final products. A weak luminescence (emission spectrum, Fig. S5, ESI†) was observed for the as-prepared $Gd(OH)CO_3 \cdot H_2O$:Eu with a quantum yield below the detection limits of our equipment (0.01), which is attributed to the amorphous nature of as-prepared materials and the presence of H_2O molecules and hydroxyl groups that serve as efficient luminescence quenchers.[9] Fig. 4 shows the room temperature photoluminescence excitation and emission spectra of mesoporous Gd_2O_3:Eu. In the excitation spectrum, a broad band with a maximum at 254 nm originates from the excitation of the oxygen-to-europium charge transfer band (CTB). The observation of the Gd^{3+} $^8S_{7/2} \rightarrow {}^6I_J$ transition located at 275 nm suggests the existence of Gd^{3+}-to-Eu^{3+} energy transfer.[10] The weak peaks in the longer wavelength region (280–420 nm) are ascribed to the direct f–f transitions within the Eu^{3+} $4f^6$ electron configuration. Upon excitation into a maximum of CTB, the mesoporous Gd_2O_3:Eu emits strong red light that covers the spectrum ranging from 580 to 720 nm due to the Eu^{3+} $^5D_0 \rightarrow {}^7F_j$ ($j = 0, 1, 2, 3, 4$) transitions. The excited-state lifetime of mesoporous Gd_2O_3:Eu prepared by our present route is also measured and evaluated around 3.3 ms, which is much longer than that of Gd_2O_3:Eu particles prepared by other methods.[11] The photoluminescence features were further quantified through the estimation of the absolute emission quantum yield. The quantum yields of 0.78 and 0.52 were acquired upon excitation at 254 and 275 nm, respectively. Such high quantum yield observed for the mesoporous Gd_2O_3:Eu was attributed to the conversion of amorphous $Gd(OH)CO_3 \cdot H_2O$ to highly crystalline phase Gd_2O_3 and the removal of luminescence quenchers such as H_2O and hydroxyl groups. Strong luminescence and mesoporous nature of our present Gd_2O_3:Eu may be particularly useful for the biological use as fluorescence labels and drug delivery vehicles. The work related to the biological use of mesoporous Gd_2O_3:Eu is in progress.

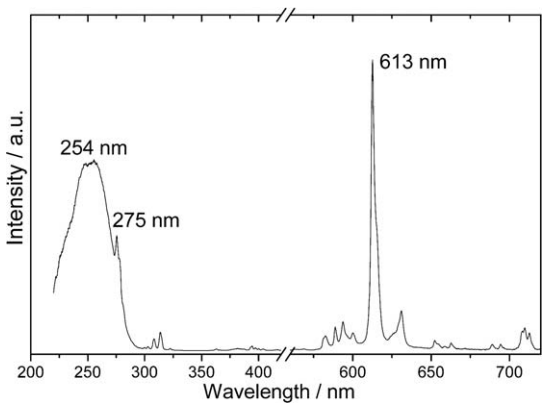

Fig. 4 Photoluminescence excitation and emission spectra of mesoporous Gd_2O_3:Eu (5 mol% doping).

In summary, we have described a solid-state thermal decomposition process for the fabrication of the mesoporous gadolinium oxides. Similarly, this approach might be applied to prepare other rare earth oxides with mesoporous structure, indicating the simplicity and generality of this novel strategy. Furthermore, the mesoporous Gd_2O_3 with lanthanide doping presents strong luminescence with a high quantum yield of 0.78. These results imply that the materials prepared by our present approach have the potential for biological uses as fluorescence labels and drug delivery carriers because of their high luminescence and mesoporous nature. The biology-related work on luminescent mesoporous Gd_2O_3:Eu is under way.

Acknowledgements

The authors gratefully acknowledge financial support from the National Natural Science Foundation of China (Grant Nos. 10874180, 50502031, 50972140 and 61077025).

Notes and references

1 (*a*) J. Bridot, A. Faure, S. Laurent, C. Riviere, C. Billotey, B. Hiba, M. Janier, V. Josserand, J. Coll, L. Elst, R. Muller, S. Roux, P. Perriat and O. Tillement, *J. Am. Chem. Soc.*, 2007, **129**, 5076; (*b*) J. Shen, L. Sun and C. Yan, *Dalton Trans.*, 2008, 5687; (*c*) K. Wong, G. Law, M. Murphy, P. Tanner, W. Wong, P. Lam and M. Lam, *Inorg. Chem.*, 2008, **47**, 5190; (*d*) S. Setua, D. Menon, A. Asok, S. Nair and M. Koyakutty, *Biomaterials*, 2010, **31**, 714; (*e*) W. Di, J. Li, N. Shirahata, Y. Sakka, M. Willinger and N. Pinna, *Nanoscale*, 2011, **3**, 1263; (*f*) F. Zhang and S. Wong, *ACS Nano*, 2010, **4**, 99; (*g*) J. Shen, L. Sun, J. Zhu, L. Wei, H. Sun and C. Yan, *Adv. Funct. Mater.*, 2010, **20**, 3707.
2 (*a*) S. Gai, P. Yang, C. Li, W. Wang, Y. Dai, N. Niu and J. Lin, *Adv. Funct. Mater.*, 2010, **20**, 1166; (*b*) Y. Zhu, T. Ikoma, N. Hanagata and S. Kaskel, *Small*, 2010, **6**, 471; (*c*) Z. Xu, C. Li, P. Ma, Z. Hou, D. Yang, X. Kang and J. Lin, *Nanoscale*, 2011, **3**, 661; (*d*) M. Liong, J. Lu, M. Kovochich, T. Xia, S. Ruehm, A. Nel, F. Tamanoi and J. Zink, *ACS Nano*, 2008, **2**, 889.
3 (*a*) Y. Wan and D. Zhao, *Chem. Rev.*, 2007, **107**, 2821; (*b*) Z. Yang, Y. Lu and Z. Yang, *Chem. Commun.*, 2009, 2270; (*c*) H. Djojoputro, X. Zhou, S. Qiao, L. Wang, C. Yu and G. Lu, *J. Am. Chem. Soc.*, 2006, **128**, 6320; (*d*) X. Zhao, X. Bao, W. Guo and F. Lee, *Mater. Today*, 2006, **9**, 32; (*e*) Q. Liu, S. Shen, G. Lu, X. Xiao, D. Mao and Y. Wang, *J. Mater. Chem.*, 2009, **19**, 8079.
4 S. Bian, J. Baltrusaitis, P. Galhotra and V. Grassian, *J. Mater. Chem.*, 2010, **20**, 8705.
5 (*a*) Y. Goto, N. Mizoshita, O. Ohtani, T. Okada, T. Shimada, T. Tani and S. Inagaki, *Chem. Mater.*, 2008, **20**, 4495; (*b*) P. Yang, S. Huang, D. Kong, J. Linand and H. Fu, *Inorg. Chem.*, 2007, **46**, 3203.
6 E. Matijevic and W. Hsu, *J. Colloid Interface Sci.*, 1987, **118**, 506.
7 S. Lechevallier, P. Lecante, R. Mauricot, H. Dexpert, J. Dexpert-Ghys, H. Kong, G. Law and K. Wong, *Chem. Mater.*, 2010, **22**, 6153.
8 (*a*) R. Petoral, F. Soderlind, A. Klasson, A. Suska, M. Fortin, N. Abrikossova, L. Selegard, P. Kall, M. Engstrom and K. Uvdal, *J. Phys. Chem. C*, 2009, **113**, 6913; (*b*) X. Bai, H. Song, G. Pan, Y. Lei, T. Wang, X. Ren, S. Lu, B. Dong, Q. Dai and L. Fan, *J. Phys. Chem. C*, 2007, **111**, 13611.
9 W. Di, X. Wang, B. Chen, S. Lu and X. Zhao, *J. Phys. Chem. B*, 2005, **109**, 13154.
10 S. Lu, J. Zhang, J. Zhang, H. Zhao, Y. Luo and X. Ren, *Nanotechnology*, 2010, **21**, 365709.
11 Y. Wang, X. Bai, T. Liu, B. Dong, L. Xu, Q. Liu and H. Song, *J. Solid State Chem.*, 2010, **183**, 2779.